



ARTICLE

Prognostic neuroimaging biomarkers of trauma-related psychopathology: resting-state fMRI shortly after trauma predicts future PTSD and depression symptoms in the AURORA study

Nathaniel G. Harnett^{1,2}, Sanne J. H. van Rooij³, Timothy D. Ely³, Lauren A. M. Lebois^{1,2}, Vishnu P. Murty⁴, Tanja Jovanovic⁵, Sarah B. Hill¹, Nathalie M. Dumornay¹, Julia B. Merker¹, Steve E. Bruce⁶, Stacey L. House⁷, Francesca L. Beaudoin⁸, Xinming An⁹, Donglin Zeng¹⁰, Thomas C. Neylan¹¹, Gari D. Clifford^{12,13}, Sarah D. Linnstaedt⁹, Laura T. Germine¹⁴, Kenneth A. Bollen¹⁵, Scott L. Rauch¹⁶, Christopher Lewandowski¹⁷, Phyllis L. Hendry¹⁸, Sophia Sheikh¹⁸, Alan B. Storrow¹⁹, Paul I. Musey Jr.²⁰, John P. Haran²¹, Christopher W. Jones²², Brittany E. Punches²³, Robert A. Swor²⁴, Meghan E. McGrath²⁵, Jose L. Pascual^{26,27}, Mark J. Seamon²⁸, Kamran Mohiuddin²⁹, Anna M. Chang³⁰, Claire Pearson³¹, David A. Peak³², Robert M. Domeier³³, Niels K. Rathlev³⁴, Leon D. Sanchez^{35,36}, Robert H. Pietrzak^{37,38}, Jutta Joormann³⁹, Deanna M. Barch⁴⁰, Diego A. Pizzagalli^{1,2}, John F. Sheridan^{41,42}, Steven E. Harte^{43,44}, James M. Elliott^{45,46,47}, Ronald C. Kessler⁴⁸, Karestan C. Koenen⁴⁹, Samuel Mclean^{9,50}, Kerry J. Ressler^{1,2} and Jennifer S. Stevens³

Neurobiological markers of future susceptibility to posttraumatic stress disorder (PTSD) may facilitate identification of vulnerable individuals in the early aftermath of trauma. Variability in resting-state networks (RSNs), patterns of intrinsic functional connectivity across the brain, has previously been linked to PTSD, and may thus be informative of PTSD susceptibility. The present data are part of an initial analysis from the AURORA study, a longitudinal, multisite study of adverse neuropsychiatric sequelae. Magnetic resonance imaging (MRI) data from 109 recently (i.e., ~2 weeks) traumatized individuals were collected and PTSD and depression symptoms were assessed at 3 months post trauma. We assessed commonly reported RSNs including the default mode network (DMN), central executive network (CEN), and salience network (SN). We also identified a proposed arousal network (AN) composed of a priori brain regions important for PTSD: the amygdala, hippocampus, mamillary bodies, midbrain, and pons. Primary analyses assessed whether variability in functional connectivity at the 2-week imaging timepoint predicted 3-month PTSD symptom severity. Left dorsolateral prefrontal cortex (DLPFC) to AN connectivity at 2 weeks post trauma was negatively related to 3-month PTSD symptoms. Further, right inferior temporal gyrus (ITG) to DMN connectivity was positively related to 3-month PTSD symptoms. Both DLPFC-AN and ITG-DMN connectivity also predicted depression symptoms at 3 months. Our results suggest that, following trauma exposure, acutely assessed variability in RSN connectivity was associated with PTSD symptom severity approximately two and a half months later. However, these patterns may reflect general susceptibility to posttraumatic dysfunction as the imaging patterns were not linked to specific disorder symptoms, at least in the subacute/early chronic phase. The present data suggest that assessment of RSNs in the early aftermath of trauma may be informative of susceptibility to posttraumatic dysfunction, with future work needed to understand neural markers of long-term (e.g., 12 months post trauma) dysfunction. Furthermore, these findings are consistent with neural models suggesting that decreased top-down cortico-limbic regulation and increased network-mediated fear generalization may contribute to ongoing dysfunction in the aftermath of trauma.

Neuropsychopharmacology (2021) 46:1263–1271; <https://doi.org/10.1038/s41386-020-00946-8>

INTRODUCTION

Traumatic experiences are unfortunately common within the United States with lifetime prevalence estimates ranging from ~60 to 90% [1, 2]. Trauma exposure can lead to acute and potentially chronic dysfunction in the form of posttraumatic stress disorder (PTSD) [3]. However, there is significant individual variability in susceptibility to PTSD, such that not all trauma exposed individuals will develop PTSD [4, 5]. Given the significant social, emotional, and financial burdens endured by individuals with

PTSD, there is a pressing need for early biosignatures of PTSD vulnerability. Such markers may both advance our understanding of PTSD biology as well as guide predictive tools for identifying susceptible individuals. Further, these findings may impact early interventions and treatments to ultimately attenuate the risk and debilitating consequences of the disorder.

Neuroimaging-based markers of PTSD susceptibility have begun to emerge as a potential avenue for the expedited development of novel early identification and intervention tools. Although many

^aA full list of authors and their affiliations appears at the end of the paper.

Correspondence: Nathaniel G. Harnett (nharnett@mclean.harvard.edu) or Jennifer S. Stevens (jennifer.stevens@emory.edu)

Received: 3 November 2020 Revised: 12 December 2020 Accepted: 16 December 2020

Published online: 21 January 2021

individuals self-report heightened stress symptoms in the acute aftermath of trauma, a substantial proportion of traumatized individuals do not go on to develop PTSD, such that self-reports in the acute phase are not always predictive of future PTSD [6, 7]. Although neuroimaging cannot currently replace traditional subjective markers of stress, quantifiable neural markers, such as those identified with neuroimaging, may provide relevant alternative information for identifying future PTSD risk when assessed during the peritraumatic period. Furthermore, understanding neural markers of individual variation may provide biological targets for stratification of heterogeneous symptom variation, advancing both research and clinical approaches to the clinical heterogeneity seen with PTSD [8].

Prior task-based functional magnetic resonance imaging (fMRI) studies have observed that activity within the amygdala, hippocampus, and prefrontal cortex (PFC)—when assessed acutely following trauma—can be predictive of future PTSD. These previous findings are consistent with the view that the development of PTSD reflects disruptions in fear processing and fear inhibition, which is supported by PFC—hippocampal—amygdala circuitry [9–13]. Although task-based fMRI has been used to probe cognitive processes potentially related to PTSD susceptibility, resting-state (i.e., task independent) fMRI provides another avenue towards quantifying neural markers of PTSD susceptibility. Specifically, resting-state fMRI (rs-fMRI) allows for the identification of resting-state networks (RSNs) which represent spatial distributions of synchronized fluctuations in blood oxygen level dependent fMRI responses over time. RSNs reflect spatial patterns of temporal coherence in brain activity and can be identified using standardized and well-validated procedures [14, 15]. In contrast to task-based fMRI, rs-fMRI has several advantages for clinical use given that it does not require external stimuli or presentation equipment and does not have any task demands on patients [16]. Given that trauma exposure may have acute effects on cognitive and neural function during tasks [13], rs-fMRI may have important benefits over task-based fMRI for imaging PTSD susceptibility acutely after trauma. Therefore, imaging of RSNs through rs-fMRI may be a useful tool for generating neural signatures of PTSD susceptibility.

Growing research demonstrates that chronic PTSD is associated with alterations in RSNs such as the default mode network (DMN), salience network (SN), and central executive network (CEN, also referred to as the frontoparietal control network) [17, 18]. The DMN spans the ventromedial PFC, the inferior parietal lobe, the posterior cingulate cortex, and the precuneus and is thought to reflect self-referential or mind-wandering aspects of cognition [19–21]. The SN spans the dorsal anterior cingulate cortex and the anterior insula, and supports attentional processes toward biologically relevant stimuli [22, 23]. Finally the CEN consists predominately of the dorsolateral PFC (DLPFC) with notable extension to inferior parietal lobule, and is thought to support high-level cognitive and executive function [24]. PTSD is associated with disruptions across all three of these functional networks (for review see [18]). For example, individuals with PTSD show greater within-network connectivity of the SN and treatment appears to reverse this increase [25–27]. Notably, it is not entirely clear whether associations between PTSD and the DMN, SN, and CEN are specific to PTSD or reflect broader stress-related psychopathology. Depression emerges equally often as PTSD after trauma, and the two disorders are highly comorbid [28]. Similar to PTSD, depression has been associated with alterations in functional connectivity of important RSNs such as the DMN and SN [29], as well as alterations in subcortical connectivity [30]. This raises the possibility that neural correlates of PTSD susceptibility post-trauma may overlap with correlates of depression susceptibility. Characterizing disorder-specific or psychopathology-general circuits is critical for a more complete understanding of the neurobiology of psychiatric disorders. However, limited research to date has investigated how

these RSNs may be related to or predict susceptibility to either PTSD or depression following trauma.

Notably, limited prior work has investigated RSNs in the early aftermath (~2 weeks) of trauma to determine their subsequent relationship with future PTSD symptoms. Previous research in individuals scanned within 2–84 days after trauma has found that variation in region-of-interest-based DMN connectivity with brain regions such as the amygdala and medial PFC is predictive of later PTSD [31–33]. The findings have been mixed such that some have observed greater DMN and amygdala/mPFC coupling associated with greater PTSD [31] while others have observed positive coupling is associated with reduced PTSD [32, 33]. These previous investigations utilized region of interest seeds and thus did not model the entire spatial extent of the DMN or other RSNs which may contribute to the mixed results. The lack of such investigations is a critical gap in our understanding of the neurobiology of PTSD development and more work is needed to better understand how variations in cognitive brain networks may play a role in susceptibility to the disorder. Specifically, although initial relevant evidence suggests that altered within-network connectivity of the DMN, SN, and CEN is associated with early PTSD, investigations assessing network-based susceptibility in the early acute posttrauma period, and among a well-powered and representative participant cohort, are needed.

It is therefore still an open question as to whether RSN alterations occurring early after trauma exposure are predictive of future PTSD development. Therefore, in the present study, we investigated rs-fMRI markers of posttraumatic stress symptom development. We hypothesized that RSN connectivity assessed acutely (~2 weeks) post trauma would predict subsequent PTSD symptom severity assessed at 3 months post trauma. Based on prior findings in chronic PTSD, we predicted greater PTSD symptom severity (at 3 months post trauma) would be associated with decreased connectivity between top-down regulatory regions (e.g., CEN and DMN). In addition to the cortical RSNs that have predominated prior work, we predicted that functional connectivity of subcortical regions, such as the amygdala and hippocampus, may be important to PTSD susceptibility. The amygdala and hippocampus are critical for fear learning and expression processes and show dysfunctional activity [34–36] and disrupted functional connectivity with regulatory regions in individuals with PTSD [37–39]. We therefore predicted greater connectivity among regions supporting threat-related attention and responses (e.g., SN and subcortical regions), and less connectivity between subcortical regions and CEN. Finally, we anticipated that these relationships would be specific to PTSD symptoms and the same relationship would not be observed with depressive symptoms.

METHODS AND MATERIALS

Participants

Participants were recruited from emergency departments (EDs) across the United States as part of the AURORA study, an ongoing multisite longitudinal study of adverse neuropsychiatric sequelae (U01 MH110925, [40]). For study inclusion, participants were required to have experienced a traumatic event that brought them to the ED. Participants were automatically qualified for study enrollment if exposed to: motor vehicle collision, physical assault, sexual assault, fall >10 feet, or mass casualty incidents. Other trauma exposures were also qualifying if: (a) the individual responded endorsed the exposure as involving actual or threatened serious injury, sexual violence, or death, either by direct exposure, witnessing, or learning about it and (b) the assessing research assistant agreed that the exposure was a plausible qualifying event. Participants with a moderate or severe traumatic brain injury were not included in the present study. rs-fMRI data from 161 participants were available. Eleven participants

Table 1. Demographic information.

Variable	Count (%) / mean (SD)
Sex	
Male	33 (30%)
Female	76 (70%)
Age	
Years	35.31 (12.97)
Race/ethnicity	
Hispanic/Latin American	17 (16%)
White-American	34 (31%)
Black-American	53 (49%)
"Other" American	5 (4%)
Employment	
Employed	69 (63%)
Retired	3 (3%)
Homemaker	3 (3%)
Student	5 (4%)
Unemployed/disabled/other	23 (21%)
No response	6 (6%)
Income	
<\$19,001	28 (25%)
\$19,001–\$35,000	29 (27%)
\$35,001–\$50,000	16 (15%)
\$50,001–\$75,000	11 (10%)
\$75,001–\$100,000	6 (6%)
>\$100,000	11 (10%)
No response	8 (7%)
PCL-5 total scores	
2 Weeks (<i>n</i> = 100)	28.71 (17.10)
3 Months (<i>n</i> = 109)	23.30 (16.83)
PROMIS depression scores	
2 Weeks (<i>n</i> = 104)	54.18 (9.81)
3 Months (<i>n</i> = 109)	53.19 (10.88)
<i>PCL-5</i> PTSD Symptom Checklist for DSM-V, <i>PROMIS</i> Patient-Reported Outcomes Measurement Information System.	

were excluded for MRI issues (one excluded for incomplete data, one excluded due to falx calcification, and nine excluded due to motion criteria described in the Supplementary Information). The analysis focused on acute rs-fMRI data as predictive of future PTSD symptoms. Thus, of the remaining 150 participants, a total of 109 participants who had complete 3-month PTSD assessments (the furthest available timepoint) were retained. Participants were recruited from twenty-two EDs within the Northeast, Southern, mid-Atlantic, or Midwest region of the United States. Participants completed MRI within ~2 weeks of recruitment ($M = 17.91$ days, $SD = 5.82$ days) at Emory University, McLean Hospital, Temple University, or Wayne State University. General exclusion criteria for the study are detailed in a prior report [40]. Additional MRI exclusion criteria included metal or ferromagnetic implants, unwillingness to complete MRI, history of seizures or epilepsy, history of Parkinson's disease, dementia, or Alzheimer's disease, and/or current pregnancy. Participant demographic information is presented in Table 1. Participants were largely admitted to the ED for a motor vehicle collision (78%) and additional information is available in the Supplementary Materials (Tables S1, S2). All participants gave written informed consent as approved by each study site's Institutional Review Board.

Psychometric assessment

PTSD symptoms were assessed using the PTSD Symptom Checklist for DSM-V (PCL-5). The PCL-5 is a 20 item self-report questionnaire that assesses the presence and severity of various posttraumatic stress symptoms [41]. Participants rated symptoms on a scale of 0 (not at all) to 4 (extremely) for the severity of each symptom. Depression symptoms were assessed using the Patient-Reported Outcomes Measurement Information System (PROMIS) Depression instrument [42]. The PROMIS questionnaire (short form 8b) has eight-items evaluating depressive symptom frequency scored from 1 (never) to 5 (always). A raw total score was computed from summing the individual items and then converted to a T-score. Both the PCL-5 and the PROMIS were administered at ~2 weeks (i.e., about the time of the MRI) and 3 months post trauma to assess symptoms over the past 2 weeks and past 30 days respectively. Further, although not the focus of the present report, participants also provided medication usage at ~2 weeks post trauma, as well as completed assessments of substance use frequency in the past 2 weeks through the PhenX toolkit [43] (Table S3).

Magnetic resonance imaging

Full details on image acquisition and processing are available in the Supplementary Material. Briefly, rs-fMRI data (TR = 2.36 s, 230 volumes, 9:05 min scan time, eyes open) were acquired on four separate Siemens 3-Tesla MRI systems using largely harmonized scan sequences (Table S4) and were preprocessed using a standardized pipeline via the FMRIPREP software package (detailed in the Supplementary Material, sitewise quality control metric comparisons detailed in Fig. S1). The processed rs-fMRI data were included in a group-level independent components analysis using FSL's Multivariate Exploratory Linear Optimized Decomposition into Independent Components (MELODIC) framework to identify RSNs [44]. A total of 28 RSNs were automatically estimated through MELODIC. Five RSNs including the DMN, SN, both left (l) and right (r) CEN, and a network comprising a priori subcortical regions of interest that spanned the amygdala, hippocampus, mamillary bodies, midbrain, and pons—regions thought to be critical to the pathology of PTSD—that we refer to here as the "arousal network (AN)" were included in our analyses (Fig. 1). Participant-specific RSN timeseries and associated RSN spatial maps were obtained using dual regression [45, 46]. Briefly, each group-level RSN spatial map was regressed into each participant's 4D dataset to obtain participant-specific RSN timeseries. The timeseries were then used as regressors in a general linear model for each participants 4D dataset to derive participant-specific spatial maps for each RSN. The participant-level spatial maps describe the connectivity strength (as a parameter estimate) between each voxel and the participant RSN timeseries. The resultant voxelwise maps can be used to investigate "network-to-node" connectivity patterns [46]. Between-network connectivity was indexed using z-transformed Pearson correlation coefficients between each of the five a priori networks (ten total pairs).

Statistical analyses

Statistical analyses were completed using IBM SPSS version 24 and the Analysis of Functional NeuroImages (AFNI) software package [47]. Network-to-node connectivity analyses were conducted using multiple linear regressions in AFNI's 3dttest++ to assess voxelwise functional connectivity for each a priori RSN as a function of PCL-5 scores at 3 months post trauma (five models total). Initial analyses focused on parsimonious models and only included dummy-coded covariates to model site/scanner effects. A gray matter mask that included subcortical areas was applied to the data. Cluster-based thresholding implemented in 3dttest++ was used to correct for multiple comparisons. Specifically, we completed permutation testing (10,000 permutations) from the

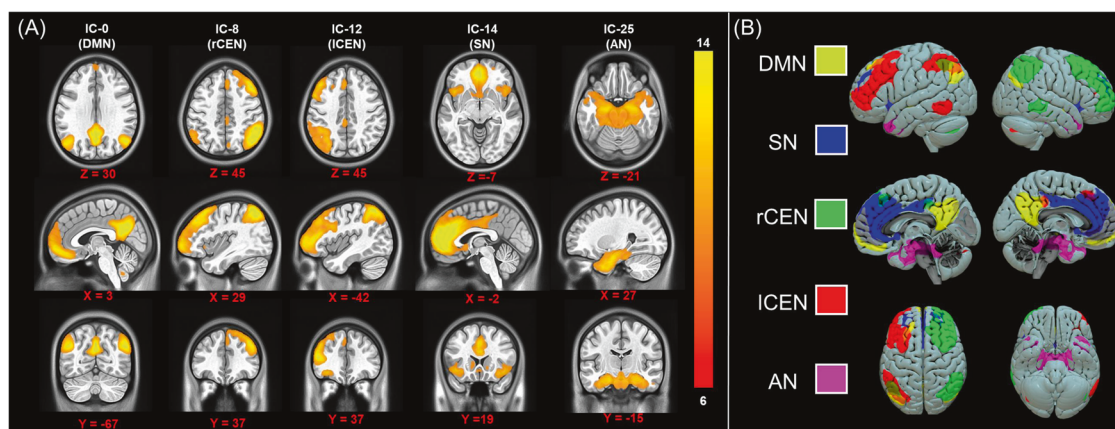


Fig. 1 Resting-state networks. Group-level independent components (IC) analysis was completed to identify resting-state networks (RSNs) of interest. We identified components that reflect the default mode network (DMN), salience network (SN), left (l) and right (r) central executive networks (CEN), and an arousal network (AN). The spatial maps for each IC/RSN are shown in the left panel (A) and resampled to 1 mm³ resolution for visualization. The right panel (B) shows a 3D visualization of each IC/RSN.

Table 2. Network-to-node connectivity associated with 3-month posttraumatic stress severity.

Structure (Network)	Hemisphere	Z-statistic	Volume	Coordinates (MNI)		
				X	Y	Z
Inferior temporal gyrus (Default mode network)	Right	4.69	k = 39 (312 mm ³)	47	-63	-9
Dorsolateral prefrontal cortex (Arousal network)	Left	-4.79	k = 30 (240 mm ³)	-47	11	27

Location, Z-statistic, cluster extent (k) (2³ mm grid spacing), volume, and Montreal Neurological Institute (MNI) coordinates of the peak voxel for clusters that showed a significant ($\alpha = 0.05$; corrected) relationship with 3-month PCL-5 (PTSD Checklist for DSM-V) scores.

residuals of each multiple linear regression to derive autocorrelation function parameters and define the minimum cluster extent at a cluster forming threshold of $p = 0.001$ ($p = 0.005/5$ comparisons) to maintain $\alpha = 0.05$. Between-network connectivity was included in multiple linear regressions with dummy-coded covariates for scanner within SPSS (one model per connection). Sensitivity analyses for significant associations were completed to determine if these effects held after controlling for 2-week PCL-5 scores, or 3-month PROMIS depression scores respectively using both cluster-restricted and whole-brain analyses. Additional analyses were completed to assess the sensitivity of the effects and to examine if the observed effects also differed by subject characteristics and are detailed in the Supplementary Information.

RESULTS

Participant demographics and psychological characteristics
 PCL-5 scores at 3 months were correlated with PCL-5 scores at 2 weeks ($r = 0.62, p < 0.001$), PROMIS depression scores at 2 weeks ($r = 0.80, p < 0.001$), and PROMIS depression scores at 3 months ($r = 0.79, p < 0.001$). These results suggest that posttraumatic outcomes were highly comorbid in the relatively early post-trauma stages.

Network-to-node connectivity and posttraumatic dysfunction
 The AN and the DMN showed significant network-to-node connectivity relationships with 3-month PCL-5 scores (Table 2). Greater dorsolateral PFC (DLPFC) to AN connectivity was associated with reduced PCL-5 scores (Fig. 2A). Further, inferior temporal gyrus (ITG) to DMN connectivity was associated with

higher PCL-5 scores (Fig. 2B). We further assessed if the present relationships were specific to PTSD symptoms or were also predictive of later depression using the functional connectivity values extracted from the significant clusters in the whole-brain analysis. Both DLPFC-AN connectivity [$t(104) = -3.99, \beta = -0.37, p < 0.001$] and ITG-DMN connectivity [$t(104) = 3.75, \beta = 0.35, p < 0.001$] significantly predicted PROMIS depression scores at 3 months post trauma.

Sensitivity analyses were completed to assess if the observed relationships between RSN connectivity and 3-month PCL-5 scores persisted when controlling for PCL-5 scores at 2 weeks or PROMIS depression scores at 3 months (described in the Supplementary Material). The cluster-restricted analyses (from the prior whole-brain analyses) revealed that DLPFC-AN connectivity was associated with 3-month PCL-5 scores when controlling for 2-week symptoms, whereas ITG-DMN connectivity was not. Additionally, ITG-DMN connectivity was associated with 3-month PCL-5 scores when controlling for 3-month depression symptoms, but DLPFC-AN connectivity was not. Exploratory whole-brain analyses that controlled for 2-week PCL-5 symptoms revealed positive associations between AN connectivity to the postcentral and visual gyri and 3-month PCL-5 symptoms (Table S5).

Between-network connectivity and posttraumatic stress
 Multiple regression analyses were completed to assess the relationship among between-network connectivity strengths (i.e., network to network connectivity) and PCL-5 scores. No significant associations were observed. These results suggest that connectivity strengths between full networks are not reflective of susceptibility to heightened PTSD symptoms at 3 months posttrauma.

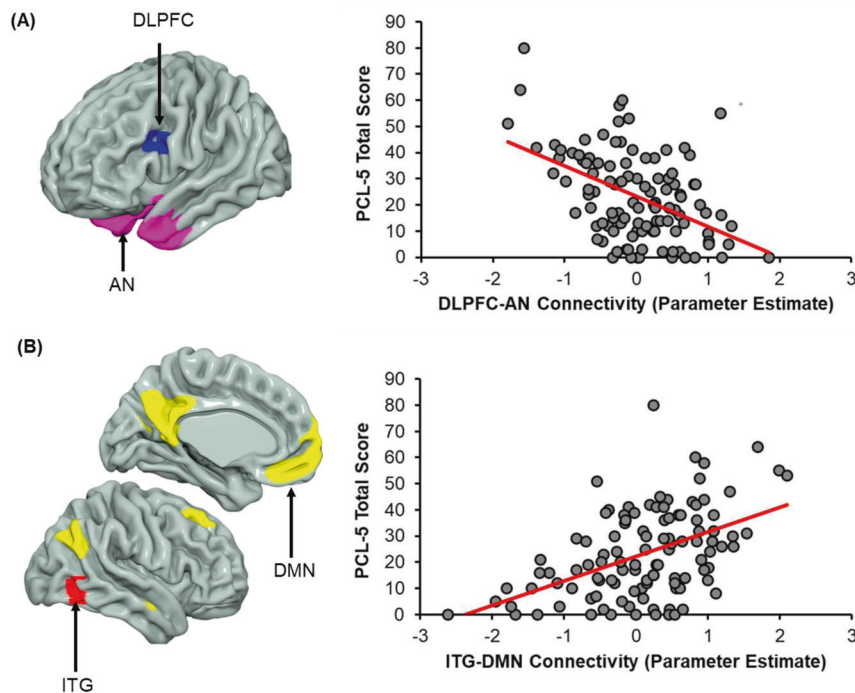


Fig. 2 Network-to-node connectivity of the default mode and arousal networks vary with 3-month posttraumatic stress severity. **A** Multiple regression analyses revealed connectivity between the left dorsolateral prefrontal cortex (DLPFC; blue) and the arousal network (AN; pink) varied inversely with 3-month PCL-5 scores. **B** Conversely, connectivity between the right inferior temporal gyrus (ITG; red) and the default mode network (DMN; yellow) was positively related to PCL-5 scores assessed 3 months post trauma. Scatterplots are not inferential but are included to illustrate the relationship between network-to-node connectivity and PCL-5 scores. Dots represent individual participant scores for connectivity (average of the cluster) and PCL-5 total score. Solid red lines represent the linear line of best fit.

Participant-specific factors, connectivity, and posttraumatic stress. Consistent with recent calls to consider demographic differences in the neural substrates of psychiatric disorders [48, 49], we completed exploratory analyses to investigate if the observed relationships varied between sex/gender, race/ethnicity, and site (described in the Supplementary Information). However, we note limited samples were available for some of the stratified analyses and the sample was unbalanced with regards to gender (70% women) and race/ethnicity (49% Black-American, 31% White-American) which may impact these exploratory analyses (see Table 1). We observed potential sex differences such that, although ITG-DMN connectivity predicted PCL-5 scores in men and women separately, DLPFC-AN connectivity did not predict PTSD symptoms in men. Further, both DLPFC-AN and ITG-DMN connectivity were generally predictive of PTSD symptoms across racial groups (i.e., Hispanic-American, White-American, and Black-American) assessed. Additionally, despite ~50% of participants having reported hitting their head during the trauma, the DLPFC-AN and ITG-DMN with 3-month PTSD associations were observed in both potentially concussed versus non-concussed individuals.

DISCUSSION

Individual variability in PTSD susceptibility is a significant barrier to enacting early treatment approaches for the disorder. Specifically, it is difficult to predict which individuals are most likely to show long-term dysfunction following trauma. Several clinical studies of early interventions have proved unfruitful, partially due to such variability [50–53]. Identification of neural markers associated with variability in PTSD susceptibility may facilitate development of predictive analytics to quickly identify at-risk individuals who might benefit from intervention. Given the relative ease of data acquisition and standardization in data processing, RSNs may be

well-suited to yield potential neural signatures of risk for PTSD. In the current investigation of RSNs in recently traumatized individuals, greater positive coupling of the right ITG to the DMN, and of the left DLPFC to the AN, were predictive of later PTSD symptom severity at 3 months post trauma. Contrary to our hypotheses, these connectivity patterns were not specific to PTSD and were also tied to posttraumatic depression symptom severity which suggests that disruptions in functional connectivity may be related to general posttraumatic dysfunction. The present findings shed important new light on the neural basis of the development of posttraumatic pathology and provide critical insight into the utility RSNs for early assessment of PTSD susceptibility.

Our analyses revealed that positive coupling of the left DLPFC to AN connectivity was associated with reduced PTSD/depression symptoms at 3 months post trauma. These findings are consistent with a recent prospective investigation showing DLPFC-amygdala connectivity in the acute phase following trauma was tied to PTSD symptoms [54]. The DLPFC is also a part of the CEN, and thus these connectivity patterns may potentially reflect some variation in between-network connectivity or communication. In the present study, the AN was comprised of the amygdala, hippocampus, and mammillary bodies, midbrain, and pons, which are regions necessary for the acquisition, behavioral expression, and extinction of fear [55–58]. Importantly, the DLPFC is thought to support cognitive-affective processes to aid in the top-down regulation of the emotional response through functional connections with regions of the AN [59, 60]. In fact, recent neuromodulation studies have noted increased DLPFC activation and connectivity with the amygdala following neurofeedback in individuals with PTSD [61]. Further, the DLPFC is a common site for neurostimulation studies (i.e., transcranial magnetic stimulation) of depression [62] and may be a promising candidate for anxiety and trauma-related disorder treatment due to concurrent attenuation of amygdala activity

following DLPFC stimulation [63–65]. Taken together with the prior literature, the inverse relationship between DLPFC-AN connectivity and PTSD severity may suggest that reductions in PTSD symptoms after trauma are partially driven by top-down regulation of the amygdala and arousal-related networks by the DLPFC. Future translational work may be able to test whether neuromodulation of left DLPFC—given its connections with arousal-related regions—in the early aftermath of trauma may promote resilience to outcomes such as PTSD or depression. Importantly, our data show that lowered DLPFC-AN connectivity is not associated with 2-week posttraumatic stress symptoms and thus selecting “high risk” individuals for neuromodulatory interventions may benefit from concurrent assessments of neural circuit features. Future work assessing the generalizability of these connections across multiple samples and trauma types would be beneficial for determining optimal targets for neuromodulation.

Our initial analyses revealed that right ITG to DMN connectivity at 2 weeks post trauma was predictive of PTSD severity at 3 months post trauma, and the same connectivity pattern was also predictive of 2-week PTSD severity (described in the supplement). These data suggest that high ITG-DMN connectivity is predictive of a persistent aspect of PTSD symptoms such that individuals who have relatively high PTSD symptoms in the early phase after trauma are likely to show high symptoms in the later stages of trauma [6, 66]. The DMN is a highly replicable spatial pattern of intrinsic functional connectivity between the ventromedial PFC, posterior cingulate cortex, and inferior parietal lobule [15, 67, 68]. Each of these regions are implicated in important affective processes such as fear learning [69], and the DMN itself is thought to play a significant role in emotional memory and regulation processes [70, 71]. Further, the ITG lays along the ventral visual processing stream and may play a role in visual recognition and memory processes (for review, see [72]). Some data suggests the ITG may also be involved in envisioning future emotional events [73]. One interpretation of the present findings is that greater ITG-DMN connectivity in the early weeks after trauma exposure supports formation, consolidation, and retrieval of emotional, traumatic memories. The facilitation of trauma memory retrieval may then contribute to the pattern of persistently high PTSD symptoms, consistent with “overconsolidation” theories [74]. An alternative possibility is that these patterns are contributing to overgeneralization processes that are observed in individuals with PTSD [75–77]. Prior work suggests ITG activity, as part of the ventral visual stream, may reflect broad, high-level representations of stimuli (e.g., “objects” or “scenes”) [78]. Recent findings indicate fear overgeneralization may occur acutely following trauma exposure [13] and greater neural activity within regions of the DMN, AN, and ventral visual stream have been associated with fear generalization in individuals with chronic PTSD [76, 79]. Future work is needed to further assess whether ITG to DMN connectivity may be related to overconsolidation, overgeneralization, or another disrupted cognitive process relevant to trauma.

Several limitations to the current study should be noted. We note that the current results do not suggest neuroimaging markers can replace typical assessments of psychiatric symptoms, but instead that the findings illustrate that key brain networks partially underlie variability in future expression of posttraumatic symptoms. Relatedly, we further note that it is difficult to infer the specific functions of the observed RSNs. Importantly, it remains somewhat unclear whether the RSN patterns observed in the present study develop early after the trauma or may be true pre-trauma vulnerability factors. Without collection of pre-trauma brain imaging data, although often difficult or infeasible, we cannot state definitively if the present results could be used to identify susceptibility to posttraumatic dysfunction in non-traumatized groups. However, the potential of the present findings to be a trait-like marker of PTSD susceptibility warrants

further investigation. Future work should seek to determine if these RSN patterns may be trait markers for posttraumatic dysfunction that may represent a signature of risk for development of PTSD following trauma exposure. In addition, although our results demonstrate the utility of RSNs for susceptibility, the observed patterns are not specific to any one type of posttraumatic outcome (e.g., PTSD or depression). This may be due in part to the high comorbidity of symptoms or shared neural substrates of symptoms in the early aftermath of trauma (~3 months). Further, identifying individuals with high comorbid symptoms may be of great benefit as these individuals may be at the most risk for long-term, chronic posttraumatic dysfunction. Nevertheless, the observed results cannot be said to be specific to a disorder in and of itself, and instead represent general cognitive-affective posttraumatic dysfunction. Finally, limited data for the present analysis was available on RSN associations with later chronic presentations (i.e., 12 months) of posttraumatic symptoms. It remains unclear if the observed associations between rs-fMRI patterns and posttraumatic symptoms is constant in the chronic phase, or if perhaps these findings diverge along different types of posttraumatic symptoms. For example, ITG-DMN connectivity may be associated with posttraumatic dysfunction in general at 12 months while DLPFC-AN connectivity may only be predictive of PTSD at 12 months. Future analyses of the growing AURORA dataset will utilize data collected at later timepoints in the chronic period to investigate these potential outcomes. Further, future research may also consider utilizing longer rs-fMRI sequences. Although ~10 min of rs-fMRI data may be sufficient to reliably measure functional connectivity [80, 81], emerging research suggests longer scans (~60 min) allow for more reliable estimates of individual brain networks [82].

In conclusion, the present study investigated the relationship between resting-state connectivity in the acute aftermath of trauma and future PTSD symptoms. We found that DLPFC-AN and ITG-DMN connectivity was related to future (i.e., 3-month) PTSD symptom severity. Notably, these connectivity patterns were also tied to 3-month depression symptoms. The present findings suggest that resting-state connectivity, assessed in the early aftermath of trauma, is related to later posttraumatic dysfunction. Further, these data suggest rs-fMRI and assessment of RSNs may provide for useful neural signatures of trauma and stress-related dysfunction.

FUNDING AND DISCLOSURE

This research was supported by the National Institute of Mental Health K00 MH119603, K01 MH118467, and U01 MH110925, the US Army Medical Research and Materiel Command, The One Mind Foundation, and The Mayday Fund. DAP has received consulting fees from Akili Interactive Labs, BlackThorn Therapeutics, Boehringer Ingelheim, Posit Science, and Takeda Pharmaceuticals, as well as an honorarium from Alkermes for activities unrelated to the current project. KJR has received consulting income from Alkermes and Takeda, research support from NIH, Genomind and Brainsway, and he is on scientific advisory boards for Janssen and Verily, all of which are unrelated to the present work. RCK has received support for his epidemiological studies from Sanofi Aventis; was a consultant for Datastat, Inc., Sage Pharmaceuticals, and Takeda. CWJ has received funding from Roche Diagnostics, AstraZeneca, Janssen, and Hologic Inc. JME reports support from the National Institutes of Health (NIH) through Grant Numbers R01HD079076 and R03HD094577; Eunice Kennedy Shriver National Institute of Child Health & Human Development; National Center for Medical Rehabilitation Research. SS has received funding from the Florida Medical Malpractice Joint Underwriter’s Association Dr. Alvin E. Smith Safety of Healthcare Services Grant; the NIH/NIA-funded Jacksonville Aging Studies Center (JAX-

ASCENT; R33AG05654); and the Florida Blue Foundation. The authors declare no competing interests.

ACKNOWLEDGEMENTS

The authors would like to thank Rebecca Price, Adam Hively, Saswati Data, Suraj Oomman, and the other members of the UNC Institute for Trauma Recovery for their efforts and aide in this research. We would also like to thank research staff at McLean Hospital, Emory University, Temple University, and Wayne State University for their efforts and aide. We further express our gratitude to the participants and their families for their willingness to participate in this research.

AUTHOR CONTRIBUTIONS

Design and conceptualization of study: RCK, KCK, SM, and KJR. Data acquisition, recruitment, and logistics: SBH, NMD, JBM, SEB, SLH, FLB, XA, DZ, TCN, GDC, SDL, KAB, SLR, CL, PLH, SS, ABS, PIM Jr., JPH, CWJ, BEP, RAS, MEM, JLP, MJS, KM, AMC, CP, DAP, RMD, NKR, and LDS. Data processing and statistical analyses: NGH, SVR, TDE, JSS. Data interpretation NGH, SVR, TDE, LAML, VPM, TJ, KJR, and JSS. Drafting of the paper: NGH, SVR, LAML, VPM, TJ, KJR, and JSS. All authors revised the paper critically for important intellectual context and agree to be accountable for all aspects of the work in ensuring that questions related to the accuracy or integrity of any part of the work are appropriately investigated and resolved.

ADDITIONAL INFORMATION

Supplementary Information accompanies this paper at (<https://doi.org/10.1038/s41386-020-00946-8>).

Publisher's note Springer Nature remains neutral with regard to jurisdictional claims in published maps and institutional affiliations.

REFERENCES

- Kessler RC, Sonnega A, Bromet E, Hughes M, Nelson CB. Posttraumatic stress disorder in the National Comorbidity Survey. *Arch Gen Psychiatry*. 1995;52:1048–60.
- Kilpatrick DG, Resnick HS, Milanak ME, Miller MW, Keyes KM, Friedman MJ. National estimates of exposure to traumatic events and PTSD prevalence using DSM-IV and DSM-5 criteria. *J Trauma Stress*. 2013;26:537–47.
- American Psychiatric Association. *Diagnostic and statistical manual of mental disorders*. 5th ed. American Psychiatric Association Press, Arlington, VA; 2013.
- Galatzer-Levy IR, Anki Y, Freedman S, Israeli-Shalev Y, Roitman P, Gilad M, et al. Early PTSD symptom trajectories: persistence, recovery, and response to treatment: results from the Jerusalem trauma outreach and prevention study (J-TOPS). *PLoS ONE*. 2013;8:e70084.
- Bonanno GA, Mancini AD. Beyond resilience and PTSD: mapping the heterogeneity of responses to potential trauma. *Psychol Trauma Theory Res Pract Policy*. 2012;4:74–83.
- Galatzer-Levy IR, Huang SH, Bonanno GA. Trajectories of resilience and dysfunction following potential trauma: A review and statistical evaluation. *Clin Psychol Rev*. 2018;63:41–55.
- Bryant RA, Creamer M, O'Donnell M, Silove D, McFarlane AC, Forbes D. A comparison of the capacity of DSM-IV and DSM-5 acute stress disorder definitions to predict posttraumatic stress disorder and related disorders. *J Clin Psychiatry*. 2015;76:391–7.
- Galatzer-Levy IR, Bryant RA. 636,120 ways to have posttraumatic stress disorder. *Perspect Psychol Sci*. 2013;8:651–62.
- van Rooij SJH, Stevens JS, Ely TD, Hinrichs R, Michopoulos V, Winters SJ, et al. The role of the hippocampus in predicting future posttraumatic stress disorder symptoms in recently traumatized civilians. *Biol Psychiatry*. 2018;84:106–15.
- Stevens JS, Kim YJ, Galatzer-Levy IR, Reddy R, Ely TD, Nemeroff CB, et al. Amygdala reactivity and anterior cingulate habituation predict posttraumatic stress disorder symptom maintenance after acute civilian trauma. *Biol Psychiatry*. 2017;81:1023–9.
- McLaughlin KA, Busso DS, Duys A, Green JG, Alves S, Way M, et al. Amygdala response to negative stimuli predicts PTSD symptom onset following a terrorist attack. *Depress Anxiety*. 2014;31:834–42.
- Admon R, Lubin G, Stern O, Rosenberg K, Sela L, Ben-Ami H, et al. Human vulnerability to stress depends on amygdala's predisposition and hippocampal plasticity. *Proc Natl Acad Sci USA*. 2009;106:14120–5.

- Harnett NG, Ference EW, Wood KH, Wheelock MD, Knight AJ, Knight DC. Trauma exposure acutely alters neural function during Pavlovian fear conditioning. *Cortex*. 2018;109:1–13.
- Beckmann CF, DeLuca M, Devlin JT, Smith SM. Investigations into resting-state connectivity using independent component analysis. *Philos Trans R Soc B Biol Sci*. 2005;360:1001–13.
- Damoiseaux JS, Rombouts SARB, Barkhof F, Scheltens P, Stam CJ, Smith SM, et al. Consistent resting-state networks across healthy subjects. *Proc Natl Acad Sci USA*. 2006;103:13848–53.
- Fox MD, Greicius M. Clinical applications of resting state functional connectivity. *Front Syst Neurosci*. 2010;4:19.
- Menon V. Large-scale brain networks and psychopathology: a unifying triple network model. *Trends Cogn Sci*. 2011;15:483–506.
- Akiki TJ, Averill CL, Abdallah CG. A network-based neurobiological model of PTSD: evidence from structural and functional neuroimaging studies. *Curr Psychiatry Rep*. 2017;19:81.
- Raichle ME, MacLeod AM, Snyder AZ, Powers WJ, Gusnard DA, Shulman GL. A default mode of brain function. *Proc Natl Acad Sci USA*. 2001;98:676–82.
- Buckner RL, Andrews-Hanna JR, Schacter DL. The brain's default network: anatomy, function, and relevance to disease. *Ann NY Acad Sci*. 2008;1124:1–38.
- Poerio GL, Sormaz M, Wang HT, Margulies D, Jefferies E, Smallwood J. The role of the default mode network in component processes underlying the wandering mind. *Soc Cogn Affect Neurosci*. 2017;12:1047–62.
- Dosenbach NUF, Fair DA, Miezin FM, Cohen AL, Wenger KK, Dosenbach RAT, et al. Distinct brain networks for adaptive and stable task control in humans. *Proc Natl Acad Sci USA*. 2007;104:11073–8.
- Seeley WW, Menon V, Schatzberg AF, Keller J, Glover GH, Kenna H, et al. Dissociable intrinsic connectivity networks for salience processing and executive control. *J Neurosci*. 2007;27:2349–56.
- Seeley WW, Menon V, Schatzberg AF, Keller J, Glover GH, Kenna H, et al. The organization of the human cerebral cortex estimated by intrinsic functional connectivity. *J Neurophysiol*. 2011;106:1125–65.
- Abdallah CG, Averill CL, Ramage AE, Averill LA, Goktas S, Nemati S, et al. Salience network disruption in U.S. army soldiers with posttraumatic stress disorder. *Chronic Stress*. 2019;3:247054701985046.
- Abdallah CG, Averill CL, Ramage AE, Averill LA, Alkin E, Nemati S, et al. Reduced salience and enhanced central executive connectivity following PTSD treatment. *Chronic Stress*. 2019;3:247054701983897.
- Koch SBJ, van Zuiden M, Nawijn L, Frijling JL, Veltman DJ, Olf M. Aberrant resting-state brain activity in posttraumatic stress disorder: a meta-analysis and systematic review. *Depress Anxiety*. 2016;33:592–605.
- Rytwinski NK, Scur MD, Feeny NC, Youngstrom EA. The co-occurrence of major depressive disorder among individuals with posttraumatic stress disorder: a meta-analysis. *J Trauma Stress*. 2013;26:299–309.
- Mulders PC, van Eijndhoven PF, Schene AH, Beckmann CF, Tendolcar I. Resting-state functional connectivity in major depressive disorder: a review. *Neurosci Biobehav Rev*. 2015;56:330–44.
- Cullen KR, Westlund MK, Klimes-Dougan B, Mueller BA, Hourai A, Eberly LE, et al. Abnormal amygdala resting-state functional connectivity in adolescent depression. *JAMA Psychiatry*. 2014;71:1138–47.
- Lanius RA, Bluhm RL, Coupland NJ, Hedgeson KM, Rowe B, Théberge J, et al. Default mode network connectivity as a predictor of post-traumatic stress disorder symptom severity in acutely traumatized subjects. *Acta Psychiatr Scand*. 2010;121:33–40.
- Zhou Y, Wang Z, Qin L-d, Wan JQ, Sun Y-W, Su S-S, et al. Early altered resting-state functional connectivity predicts the severity of post-traumatic stress disorder symptoms in acutely traumatized subjects. *PLoS ONE*. 2012;7:e46833.
- Qin L-D, Wang Z, Sun YW, Wan JQ, Su SS, Zhou Y, et al. A preliminary study of alterations in default network connectivity in post-traumatic stress disorder patients following recent trauma. *Brain Res*. 2012;1484:50–6.
- Milad MR, Pitman RK, Ellis CB, Gold AL, Shin LM, Lasko NB, et al. Neurobiological basis of failure to recall extinction memory in posttraumatic stress disorder. *Biol Psychiatry*. 2009;66:1075–82.
- Hayes JP, Hayes SM, Mikesis AM. Quantitative meta-analysis of neural activity in posttraumatic stress disorder. *Biol Mood Anxiety Disord*. 2012;2:9.
- Knight DC, Smith CN, Cheng DT, Stein EA, Helmstetter FJ. Amygdala and hippocampal activity during acquisition and extinction of human fear conditioning. *Cogn Affect Behav Neurosci*. 2004;4:317–25.
- Stevens JS, Jovanovic T, Fani N, Ely TD, Glover EM, Bradley B, et al. Disrupted amygdala-prefrontal functional connectivity in civilian women with posttraumatic stress disorder. *J Psychiatr Res*. 2013;47:1469–78.
- Lazarov A, Zhu X, Suarez-Jimenez B, Rutherford BR, Neria Y. Resting-state functional connectivity of anterior and posterior hippocampus in posttraumatic stress disorder. *J Psychiatr Res*. 2017;94:15–22.

39. Sripada RK, King AP, Garfinkel SN, Wang X, Sripada CS, Welsh RC, et al. Altered resting-state amygdala functional connectivity in men with posttraumatic stress disorder. *J Psychiatry Neurosci*. 2012;37:241–9.
40. McLean SA, Ressler K, Koenen KC, Neylan T, Germine L, Jovanovic T, et al. The AURORA study: a longitudinal, multimodal library of brain biology and function after traumatic stress exposure. *Mol Psychiatry*. 2020;25:283–96.
41. Weathers FW, Litz BT, Keane TM, Palmieri PA, Marx BP, Schnurr PP. The PTSD checklist for DSM-5 (PCL-5). *Natl Cent PTSD*. 2013;5:2002.
42. Pilkonis PA, Choi SW, Reise SP, Stover AM, Riley WT, Cella D. Item banks for measuring emotional distress from the patient-reported outcomes measurement information system (PROMIS[®]): depression, anxiety, and anger. *Assessment*. 2011;18:263–83.
43. Hamilton CM, Strader LC, Pratt JG, Maiese D, Hendershot T, Kwok RK, et al. The PhenX toolkit: get the most from your measures. *Am J Epidemiol*. 2011;174:253–60.
44. Smith SM, Jenkinson M, Woolrich MW, Beckmann CF, Behrens TEJ, Johansen-Berg H, et al. Advances in functional and structural MR image analysis and implementation as FSL. *Neuroimage*. 2004;23:S208–19.
45. Nickerson LD, Smith SM, Öngür D, Beckmann CF. Using dual regression to investigate network shape and amplitude in functional connectivity analyses. *Front Neurosci*. 2017;11:115.
46. Beckmann C, Mackay C, Filippini N, Smith S. Group comparison of resting-state fMRI data using multi-subject ICA and dual regression. *Neuroimage*. 2009;47:S148.
47. Cox RW. AFNI: Software for analysis and visualization of functional magnetic resonance neuroimages. *Comput Biomed Res*. 1996;29:162–73.
48. Seligowski AV, Harnett NG, Merker JB, Ressler KJ. Nervous and endocrine system dysfunction in posttraumatic stress disorder: an overview and consideration of sex as a biological variable. *Biol Psychiatry Cogn Neurosci Neuroimaging*. 2020;5:381–91.
49. Harnett NG. Neurobiological consequences of racial disparities and environmental risks: a critical gap in understanding psychiatric disorders. *Neuropsychopharmacology*. 2020. <https://doi.org/10.1038/s41386-020-0681-4>.
50. Maples-Keller JL, Post LM, Price M, Goodnight JM, Burton MS, Yasinski CW, et al. Investigation of optimal dose of early intervention to prevent posttraumatic stress disorder: a multiarm randomized trial of one and three sessions of modified prolonged exposure. *Depress Anxiety*. 2020;37:429–37.
51. Ressler KJ. Alpha-adrenergic receptors in PTSD—failure or time for precision medicine? *N Engl J Med*. 2018;378:575–6.
52. Zohar J, Fostick L, Juven-Wetzler A, Kaplan Z, Shalev H, Schreiber G, et al. Secondary prevention of chronic PTSD by early and short-term administration of escitalopram: a prospective randomized, Placebo-Controlled, double-blind trial. *J Clin Psychiatry*. 2018;79:48–54.
53. Pitman RK, Sanders KM, Zusman RM, Healy AR, Cheema F, Lasko NB, et al. Pilot study of secondary prevention of posttraumatic stress disorder with propranolol. *Biol Psychiatry*. 2002;51:189–92.
54. Belleau EL, Ehret LE, Hanson JL, Brasel KJ, Larson CL, deRoon-Cassini TA. Amygdala functional connectivity in the acute aftermath of trauma prospectively predicts severity of posttraumatic stress symptoms: Functional connectivity predicts future PTSD symptoms. *Neurobiol Stress*. 2020;12:100217.
55. van Rooij SJH, Jovanovic T. Impaired inhibition as an intermediate phenotype for PTSD risk and treatment response. *Prog Neuropsychopharmacol Biol Psychiatry*. 2019;89:435–45.
56. Milad MR, Wright CI, Orr SP, Pitman RK, Quirk GJ, Rauch SL. Recall of fear extinction in humans activates the ventromedial prefrontal cortex and hippocampus in concert. *Biol Psychiatry*. 2007;62:446–54.
57. Cheng DT, Knight DC, Smith CN, Stein EA, Helmstetter FJ. Functional MRI of human amygdala activity during Pavlovian fear conditioning: stimulus processing versus response expression. *Behav Neurosci*. 2003;117:3–10.
58. Cheng DT, Disterhoft JF, Power JM, Ellis DA, Desmond JE. Neural substrates underlying human delay and trace eyeblink conditioning. *Proc Natl Acad Sci USA*. 2008;105:8108–13.
59. Comte M, Schön D, Coull JT, Reynaud E, Khalifa S, Belzeaux R, et al. Dissociating bottom-up and top-down mechanisms in the cortico-limbic system during emotion processing. *Cereb Cortex*. 2016;26:144–55.
60. Wheelock MD, Sreenivasan KR, Wood KH, Ver Hoef LW, Deshpande G, Knight DC. Threat-related learning relies on distinct dorsal prefrontal cortex network connectivity. *Neuroimage*. 2014;102:904–12.
61. Wheelock MD, Sreenivasan KR, Wood KH, Ver Hoef LW, Deshpande G, Knight DC. The neurobiology of emotion regulation in posttraumatic stress disorder: Amygdala downregulation via real-time fMRI neurofeedback. *Hum Brain Mapp*. 2017;38:541–60.
62. Berlim MT, Van Den Eynde F, Jeff Daskalakis Z. Clinically meaningful efficacy and acceptability of low-frequency repetitive transcranial magnetic stimulation (rTMS) for treating primary major depression: a meta-analysis of randomized, double-blind and sham-controlled trials. *Neuropsychopharmacology*. 2013;38:543–51.
63. Baeken C, De Raedt R, Van Schuerbeek P, Vanderhasselt MA, De Mey J, Bossuyt A, et al. Right prefrontal HF-rTMS attenuates right amygdala processing of negatively valenced emotional stimuli in healthy females. *Behav Brain Res*. 2010;214:450–5.
64. Philip NS, Barredo J, van't Wout-Frank M, Tyrka AR, Price LH, Carpenter LL. Network mechanisms of clinical response to transcranial magnetic stimulation in posttraumatic stress disorder and major depressive disorder. *Biol Psychiatry*. 2018;83:263–72.
65. Fonzo GA, Goodkind MS, Oathes DJ, Zaiko YV, Harvey M, Peng KK, et al. PTSD psychotherapy outcome predicted by brain activation during emotional reactivity and regulation. *Am J Psychiatry*. 2017;174:1163–74.
66. Shalev AY, Gevonden M, Ratanatharathorn A, Laska E, van der Mei WF, Qi W, et al. Estimating the risk of PTSD in recent trauma survivors: results of the International Consortium to Predict PTSD (ICPP). *World Psychiatry*. 2019;18:77–87.
67. Raichle ME. The brain's default mode network. *Annu Rev Neurosci*. 2015. <https://doi.org/10.1146/annurev-neuro-071013-014030>.
68. Harrison BJ, Pujol J, López-Solà M, Hernández-Ribas R, Deus J, Ortiz H, et al. Consistency and functional specialization in the default mode brain network. *Proc Natl Acad Sci USA*. 2008. <https://doi.org/10.1073/pnas.0711791105>.
69. Goodman AM, Harnett NG, Knight DC. Pavlovian conditioned diminution of the neurobehavioral response to threat. *Neurosci Biobehav Rev*. 2018;84:218–24.
70. Pan J, Zhan L, Hu CL, Yang J, Wang C, Gu L, et al. Emotion regulation and complex brain networks: Association between expressive suppression and efficiency in the fronto-parietal network and default-mode network. *Front Hum Neurosci*. 2018;12:70.
71. Satpute AB, Lindquist KA. The default mode network's role in discrete emotion. *Trends Cogn Sci*. 2019;23:851–64.
72. Kravitz DJ, Saleem KS, Baker CI, Ungerleider LG, Mishkin M. The ventral visual pathway: an expanded neural framework for the processing of object quality. *Trends Cogn Sci*. 2013;17:26–49.
73. D'Argembeau A, Xue G, Lu ZL, Van der Linden M, Bechara A. Neural correlates of envisioning emotional events in the near and far future. *Neuroimage*. 2008. <https://doi.org/10.1016/j.neuroimage.2007.11.025>.
74. Pitman RK, Delahanty DL. Conceptually driven pharmacologic approaches to acute trauma. *CNS Spectr*. 2005;10:99–106.
75. Jovanovic T, Ressler KJ. How the neurocircuitry and genetics of fear inhibition may inform our understanding of PTSD. *Am J Psychiatry*. 2010;167:648–62.
76. Morey RA, Haswell CC, Stjepanović D, Brancu M, Beckham JC, Calhoun PS, et al. Neural correlates of conceptual-level fear generalization in posttraumatic stress disorder. *Neuropsychopharmacology*. 2020. <https://doi.org/10.1038/s41386-020-0661-8>.
77. Berg H, Ma Y, Rueter A, Kaczurkin A, Burton PC, DeYoung CG, et al. Saliency and central executive networks track overgeneralization of conditioned-fear in post-traumatic stress disorder. *Psychol Med*. 2020;1–10.
78. Norman KA, Polyn SM, Detre GJ, Haxby JV. Beyond mind-reading: multi-voxel pattern analysis of fMRI data. *Trends Cogn Sci*. 2006;10:424–30.
79. Morey RA, Dunsmoor JE, Haswell CC, Brown VM, Vora A, Weiner J, et al. Fear learning circuitry is biased toward generalization of fear associations in post-traumatic stress disorder. *Transl Psychiatry*. 2015;5:e700.
80. Tomasi DG, Shokri-Kojori E, Volkow ND. Temporal evolution of brain functional connectivity metrics: Could 7 min of rest be enough? *Cereb Cortex*. 2017;27:4153–65.
81. Shehzad Z, Kelly AMC, Reiss PT, Gee DG, Gotimer K, Uddin LQ, et al. The resting brain: unconstrained yet reliable. *Cereb Cortex*. 2009;19:2209–29.
82. Noble S, Spann MN, Tokoglu F, Shen X, Constable RT, Scheinost D. Influences on the test-retest reliability of functional connectivity MRI and its relationship with behavioral utility. *Cereb Cortex*. 2017;27:5415–29.

Nathaniel G. Harnett^{1,2*}, Sanne J. H. van Rooij³, Timothy D. Ely³, Lauren A. M. Lebois^{1,2}, Vishnu P. Murty⁴, Tanja Jovanovic⁵, Sarah B. Hill¹, Nathalie M. Dumornay¹, Julia B. Merker¹, Steve E. Bruce⁶, Stacey L. House⁷, Francesca L. Beaudoin⁸, Xinming An⁹, Donglin Zeng¹⁰, Thomas C. Neylan¹¹, Gari D. Clifford^{12,13}, Sarah D. Linnstaedt¹⁴, Laura T. Germine¹⁴, Kenneth A. Bollen¹⁵, Scott L. Rauch¹⁶, Christopher Lewandowski¹⁷, Phyllis L. Hendry¹⁸, Sophia Sheikh¹⁸, Alan B. Storrow¹⁹, Paul I. Musey Jr.²⁰, John P. Haran²¹, Christopher W. Jones²², Brittany E. Punches^{18,23}, Robert A. Sworz²⁴, Meghan E. McGrath²⁵, Jose L. Pascual^{26,27}, Mark J. Seamon²⁸, Kamran

Mohiuddin²⁹, Anna M. Chang³⁰, Claire Pearson³¹, David A. Peak³², Robert M. Domeier³³, Niels K. Rathlev³⁴, Leon D. Sanchez^{35,36}, Robert H. Pietrzak^{37,38}, Jutta Joormann³⁹, Deanna M. Barch⁴⁰, Diego A. Pizzagalli^{1,2}, John F. Sheridan^{41,42}, Steven E. Harte^{43,44}, James M. Elliott^{45,46,47}, Ronald C. Kessler⁴⁸, Karestan C. Koenen⁴⁹, Samuel Mclean^{9,50}, Kerry J. Ressler^{1,2} and Jennifer S. Stevens^{3*}

¹Division of Depression and Anxiety, McLean Hospital, Belmont, MA, USA. ²Department of Psychiatry, Harvard Medical School, Boston, MA, USA. ³Department of Psychiatry and Behavioral Sciences, Emory University, Atlanta, GA, USA. ⁴Department of Psychology, Temple University, Philadelphia, PA, USA. ⁵Department of Psychiatry and Behavioral Neurosciences, Wayne State University, Detroit, MI, USA. ⁶Department of Psychological Sciences, University of Missouri - St. Louis, Springfield, MO, USA. ⁷Department of Emergency Medicine, Washington University School of Medicine, St. Louis, MO, USA. ⁸Department of Emergency Medicine & Health Services, Policy, and Practice, Rhode Island Hospital and The Miriam Hospital, The Alpert Medical School of Brown University, Providence, RI, USA. ⁹Institute of Trauma Recovery, Department of Anesthesiology, University of North Carolina at Chapel Hill, Chapel Hill, NC, USA. ¹⁰Department of Biostatistics, Gillings School of Global Public Health, University of North Carolina at Chapel Hill, Chapel Hill, NC, USA. ¹¹Departments of Psychiatry and Neurology, University of California at San Francisco, San Francisco, CA, USA. ¹²Department of Biomedical Informatics, Emory University School of Medicine, Atlanta, GA, USA. ¹³Department of Biomedical Engineering, Georgia Institute of Technology and Emory University, Atlanta, GA, USA. ¹⁴Institute for Technology in Psychiatry, McLean Hospital, Belmont, MA, USA. ¹⁵Department of Psychology and Neuroscience, Department of Sociology, University of North Carolina at Chapel Hill, Chapel Hill, NC, USA. ¹⁶Department of Psychiatry, McLean Hospital, Belmont, MA, USA. ¹⁷Department of Emergency Medicine, Henry Ford Health System, Detroit, MI, USA. ¹⁸Department of Emergency Medicine, University of Florida College of Medicine, Jacksonville, FL, USA. ¹⁹Department of Emergency Medicine, Vanderbilt University Medical Center, Nashville, TN, USA. ²⁰Department of Emergency Medicine, Indiana University School of Medicine, Indianapolis, IN, USA. ²¹Department of Emergency Medicine, University of Massachusetts Medical School, Worcester, MA, USA. ²²Department of Emergency Medicine, Cooper Medical School of Rowan University, Camden, NJ, USA. ²³Department of Emergency Medicine, College of Medicine & College of Nursing, University of Cincinnati, Cincinnati, OH, USA. ²⁴Department of Emergency Medicine, Oakland University William Beaumont School of Medicine, Rochester, MI, USA. ²⁵Department of Emergency Medicine, Boston Medical Center, Boston, MA, USA. ²⁶Department of Surgery, Perelman School of Medicine at the University of Pennsylvania, Philadelphia, PA, USA. ²⁷Department of Neurosurgery, Perelman School of Medicine at the University of Pennsylvania, Philadelphia, PA, USA. ²⁸Division of Traumatology, Surgical Critical Care and Emergency Surgery, University of Pennsylvania, Philadelphia, PA, USA. ²⁹Department of Emergency Medicine, Einstein Medical Center, Philadelphia, PA, USA. ³⁰Department of Emergency Medicine, Jefferson University Hospitals, Philadelphia, PA, USA. ³¹Department of Emergency Medicine, Wayne State University, Detroit, MI, USA. ³²Department of Emergency Medicine, Massachusetts General Hospital, Massachusetts, MA, USA. ³³Department of Emergency Medicine, Saint Joseph Mercy Hospital, Ann Arbor, MI, USA. ³⁴Department of Emergency Medicine, University of Massachusetts Medical School-Baystate, Springfield, MA, USA. ³⁵Department of Emergency Medicine, Beth Israel Deaconess Medical Center, Boston, MA, USA. ³⁶Department of Emergency Medicine, Harvard Medical School, Boston, MA, USA. ³⁷Department of Psychiatry, Yale School of Medicine, New Haven, CT, USA. ³⁸U.S. Department of Veterans Affairs National Center for Posttraumatic Stress Disorder, VA Connecticut Healthcare System, West Haven, CT, USA. ³⁹Department of Psychology, Yale University, New Haven, CT, USA. ⁴⁰Department of Psychological & Brain Sciences, Washington University in St. Louis, St. Louis, MO, USA. ⁴¹Department of Biosciences and Neuroscience, OSU Wexner Medical Center, Columbus, OH, USA. ⁴²Institute for Behavioral Medicine Research, OSU Wexner Medical Center, Columbus, OH, USA. ⁴³Department of Anesthesiology, University of Michigan Medical School, Ann Arbor, MI, USA. ⁴⁴Department of Internal Medicine-Rheumatology, University of Michigan Medical School, Ann Arbor, MI, USA. ⁴⁵The Kolling Institute of Medical Research, Northern Clinical School, University of Sydney, Camperdown, NSW, Australia. ⁴⁶Faculty of Medicine and Health, University of Sydney, Camperdown, NSW, Australia. ⁴⁷Physical Therapy & Human Movement Sciences, Feinberg School of Medicine at Northwestern University, Chicago, IL, USA. ⁴⁸Department of Health Care Policy, Harvard Medical School, Boston, MA, USA. ⁴⁹Department of Epidemiology, Harvard T.H. Chan School of Public Health, Boston, MA, USA. ⁵⁰Department of Emergency Medicine, University of North Carolina at Chapel Hill, Chapel Hill, NC, USA.

Supplementary Material to “Prognostic neuroimaging biomarkers of trauma-related psychopathology: Resting state fMRI shortly after trauma predicts future PTSD and depression symptoms in the AURORA study.”

Supplementary Methods

Additional participant information

Additional information on participants is provided in Tables S1, S2, and S3 to more fully describe the present trauma-exposed sample. Within the ED, participant injury severity was assessed using the Abbreviated Injury Scale (AIS), a 6-point scale of injury by anatomical location. A standard Injury Severity Score (ISS) was obtained from the sum of squares of the highest AIS scores of the three most injured regions. Further, participants were asked to rate their subjective chances of dying as a result of the traumatic event on a scale from 0 to 10 to assess participants views on the severity of the traumatic event. Participants were also asked if they remembered hitting their head as a part of the trauma that brought them to the ED and queried for potential concussion. Potential concussion was defined as participants who a) reported hitting their head, b) reporting being “knocked-out,” experiencing “temporary amnesia,” “feeling sleepy or confused,” or endorsing 3 questions above 2 points on an adapted version of the Rivermead Post-Concussion Syndrome Questionnaire within the ED. Finally, as completed in the 2-week and 3-month assessments, participants in the ED completed the PCL-5 and PROMIS depression short form questionnaires. Participants were asked to report symptoms retrospectively from the past 30 days prior to the trauma event.

Magnetic resonance imaging

MRI data were collected across four sites with relatively harmonized acquisition parameters (Table S4). Results included in this manuscript come from preprocessing performed using FMRIPREP version stable 1.2.2 [1, 2, RRID:SCR_016216], a Nipype [3, 4, RRID:SCR_002502] based tool. Each T1w (T1-weighted) volume was corrected for INU (intensity non-uniformity) using N4BiasFieldCorrection v2.1.0 [5] and skull-stripped using antsBrainExtraction.sh v2.1.0 (using the OASIS template). Brain surfaces were reconstructed using recon-all from FreeSurfer v6.0.1 [6, RRID:SCR_001847], and the brain mask estimated previously was refined with a custom variation of the method to reconcile ANTs-derived and FreeSurfer-derived segmentations of the cortical gray-matter of Mindboggle [21, RRID:SCR_002438]. Spatial normalization to the ICBM 152 Nonlinear Asymmetrical template version 2009c [7, RRID:SCR_008796] was performed through nonlinear registration with the antsRegistration tool of ANTs v2.1.0 [8, RRID:SCR_004757], using brain-extracted versions of both T1w volume and template. Brain tissue segmentation of cerebrospinal fluid (CSF), white-matter (WM) and gray-matter (GM) was performed on the brain-extracted T1w using fast [17] (FSL v5.0.9, RRID:SCR_002823). Functional data was slice time corrected using 3dTshift from AFNI v16.2.07 [11, RRID:SCR_005927] and motion corrected using mcflirt (FSL v5.0.9 [9]). This was followed by co-registration to the corresponding T1w using boundary-based registration [16] with six degrees of freedom, using bbregister (FreeSurfer v6.0.1). Motion correcting transformations, BOLD-to-T1w transformation and T1w-to-template (MNI) warp were concatenated and applied in a single step using antsApplyTransforms (ANTs v2.1.0) using Lanczos interpolation. Frame-wise displacement [19] was calculated for each functional run using the implementation of Nipype. ICA-based Automatic Removal Of Motion Artifacts (AROMA)

was used to generate aggressive noise regressors as well as to create a variant of data that is non-aggressively denoised [20]. Many internal operations of FMRIPREP use Nilearn [22, RRID:SCR_001362], principally within the BOLD-processing workflow. For more details of the pipeline see <https://fmriprep.readthedocs.io/en/stable/workflows.html>.

Participants were automatically excluded from analyses if greater than 15% of the rs-fMRI volumes exceeded 1 mm framewise displacement (FD). The rs-fMRI data (TR = 2.36 sec, 230 volumes, 9:05 minute scan time) were processed using ICA-AROMA as part of the FMRIPREP pipeline, which has been shown to handle motion artifacts in a robust, data-driven fashion that performs equal to and in some cases better than standard scrubbing or censoring procedures at the individual participant level [23, 24, but see 25]. The rs-fMRI data were further processed within the Analysis for Functional NeuroImages (AFNI) program 3dTproject by application of a bandstop filter (> 0.1 Hz) to account for physiological noise (e.g., heart rate and respiration) and censoring of non-steady state volumes identified by FMRIPREP respectively.

Given the present investigation involved pooled data from a multisite cohort, we assessed site-wise differences in data quality through four separate metrics as part of MRI-QC [26]: the AFNI Quality Index (AQI), FD, DVARS, and temporal-signal-to-noise (TSNR). AQI is a general and crude screening tool for motion or scanner artifacts in 4D datasets. AQI is calculated as an average of 1 minus the Spearman rank correlation coefficient for every volume to the median volume in the dataset. Framewise displacement is an estimation of head-movement across the dataset [27]. DVARS is calculated as the derivative of the root-mean-square variance over dataset voxels [27]. Finally, TSNR is the temporally averaged signal to noise ratio for each dataset. Site-wise statistics are provided in the supplementary results and Figure S1.

Supplementary Analyses

We completed an array of follow-up analyses designed to assess the specificity and sensitivity of the observed relationships between RSN connectivity and later posttraumatic dysfunction. Functional connectivity values from significant clusters of functional connectivity in the whole-brain analyses were extracted and used in secondary analyses with PCL-5 scores at 2-weeks and the change in PCL-5 scores between 2-weeks and 3-months to determine if the observed connections also played a role in acute PTSD symptoms or changes in PTSD symptoms over time. We further investigated whether the observed functional connectivity predicted PCL-5 scores at 3-months while controlling for 2-week PCL-5 scores. These analyses were completed at a) a voxelwise level restricted to the clusters of connectivity from the whole-brain analyses and b) at an exploratory whole-brain voxelwise level. In addition, we further investigated whether observed relationships with PCL-5 scores at 3-months post-trauma were also observed with PROMIS depression scores at 3-months post-trauma at the same analysis levels. Finally, we also completed sensitivity analyses to determine if the clusters of connectivity significantly predicted 3-month PCL-5 or PROMIS depression scores when controlling for PTSD or depression symptoms assessed within the ED.

Supplementary Results

Sitewise differences in quality assurance metrics

Sitewise differences in AQI, FD, DVARs, and TSNR are displayed in Figure S1. ANOVAs revealed a significant difference between sites in AQI [$F(3,105) = 21.80, p < 0.001$], DVARs [$F(3,105) = 4.12, p = 0.008$], and TSNR [$F(3,105) = 16.69, p < 0.001$], but no difference was observed in FD [$F(3,105) = 1.25, p = 0.29$]. Site 3 demonstrated reduced scores on AQI compared

to all other sites, and site 1 demonstrated reduced scores compared to site 4 (all $p < 0.05$). Site 3 also showed reduced DVARs compared to sites 2 and 4 (all $p < 0.05$). Finally, site 3 showed greater TSNR compared to all other sites (all $p < 0.05$).

Quality assurance metrics vary with network-to-node connectivity, but do not affect the relationship between connectivity and posttraumatic stress

In our primary analyses, site was included as a covariate in statistical models. We also performed supplementary correlation analyses to determine if the observed network-to-node connectivity patterns varied with the different quality assurance metrics. DLPFC-AN connectivity was significantly correlated with DVARs ($r = 0.25$, $p = 0.01$), TSNR ($r = -0.20$, $p = 0.03$), and AQI ($r = 0.27$, $p = 0.004$). ITG-DMN connectivity was significantly correlated with FD ($r = -0.26$, $p = 0.007$) and DVARs ($r = -0.23$, $p = 0.01$). We also observed that PCL-5 scores at 3-months post-trauma were significantly associated with FD ($r = -0.21$, $p = 0.03$), DVARs ($r = -0.26$, $p = 0.007$), and TSNR ($r = 0.20$, $p = 0.04$). Although these same metrics varied across sites, and site was included as a covariate in our models, we completed follow-up regression analyses to predict PCL-5 scores at 3-months post-trauma that included covariates for site, FD, DVARs, TSNR, and AQI with a predictor variable of network-to-node connectivity (two separate models). Even accounting for scanner and potential motion effects, 3-month PCL-5 scores varied significantly with and DLPFC-AN [$t(100) = -4.82$, $p < 0.001$, $\beta = -0.45$] and ITG-DMN [$t(100) = 5.21$, $p < 0.001$, $\beta = 0.47$] connectivity.

Follow-up analyses of network-to-node connectivity and PTSD

We assessed if the relationship between functional connectivity and PCL-5 scores were specific to the measurements at the 3-month timepoint, or if they were also related to earlier symptoms (i.e., acute posttraumatic stress) at 2-weeks after trauma. ITG-DMN connectivity [$t(95) = 4.31, p < 0.001, \beta = 0.40$], but not DLPFC-AN connectivity [$t(95) = -1.77, p = 0.08, \beta = -0.18$], varied with 2-week PCL-5 scores. Accordingly, ITG-DMN connectivity did not vary with the change in PCL-5 scores between 2-weeks and 3-months [$t(95) = 1.08, p = 0.28, \beta = 0.11$], but DLPFC-AN connectivity did vary with the change in PCL-5 scores over time [$t(95) = -3.55, p < 0.001, \beta = -0.34$].

We completed additional analyses for RSNs that significantly predicted PCL-5 scores at 3-months post-trauma, adding in a covariate for PCL-5 scores at 2-weeks post-trauma. When controlling for PCL-5 scores at 2-weeks using the extracted data from the significant clusters in the initial whole-brain analyses both ITG-DMN [$t(95) = 3.59, p < 0.001, \beta = 0.30$] and DLPFC-AN [$t(95) = -5.21, p < 0.001, \beta = -0.38$] were associated with PCL-5 scores at 3-months. Analyses restricted to the connectivity clusters from the whole-brain analyses revealed DLPFC-AN connectivity [$Z_{\text{peak}} = -4.47, p < 0.01_{\text{corrected}}, k = 20, \text{XYZ}_{\text{MNI}} = (-47, 12, 28)$] was predictive of 3-month PCL-5 scores when controlling for the scores at 2-weeks. Whole-brain analyses revealed that connectivity of the visual cortex and postcentral gyrus to the AN were also predictive of 3-month PCL-5 scores when controlling for PCL-5 scores at 2-weeks (Table S5).

Follow-up analyses of network-to-node connectivity and depression.

We completed additional analyses for RSNs that significantly predicted PCL-5 scores at 3-months post-trauma, adding in a covariate for PROMIS depression scores at 3-months post-trauma. When controlling for 3-month PROMIS depression scores using the extracted data from the significant clusters in the initial whole-brain analysis, PCL-5 [$t(103) = -3.35$, $\beta = -0.48$, $p = 0.001$] but not PROMIS depression [$t(103) = 0.09$, $\beta = 0.01$, $p = 0.93$] scores were associated with DLPFC-AN connectivity. Further, PCL-5 [$t(103) = 4.05$, $\beta = 0.57$, $p < 0.001$] but not PROMIS depression scores [$t(103) = -0.74$, $\beta = -0.10$, $p = 0.46$] were associated with ITG-DMN connectivity. Cluster-restricted analyses revealed ITG-DMN connectivity [$Z_{\text{peak}} = 3.86$, $p < 0.01_{\text{corrected}}$, $k = 9$, $XYZ_{\text{MNI}} = (47, -63, -9)$] was predictive of 3-month PCL-5 scores when controlling for the scores at 3-month PROMIS depression scores. No significant effects were observed at the whole-brain level.

Follow-up analyses of network-to-node connectivity with ED symptoms

We completed additional analyses for RSNs that significantly predicted PCL-5 scores at 3-months post-trauma, adding covariates for PTSD and depression symptoms endorsed within the ED. When controlling for pretraumatic PTSD and depression scores using the extracted data from the significant clusters in the initial whole-brain analysis, DLPFC-AN [$t(57) = -4.71$, $p < 0.001$, $\beta = -0.46$] and ITG-DMN [$t(58) = 3.57$, $p < 0.001$, $\beta = 0.38$] predicted 3-month PTSD symptoms when controlling for PTSD and depression symptoms within the ED.

Subgroup analyses

We completed subgroup analyses to investigate participant-specific factors that may impact the association between network-to-node connectivity and later posttraumatic stress symptoms. As noted in the main text, limited samples were available for analyses on gender and race/ethnicity effects which should be considered in interpreting results from these exploratory analyses. DLPFC-AN [$t(71) = -5.42$, $\beta = -0.54$, $p < 0.001$] and ITG-DMN [$t(71) = 5.06$, $\beta = 0.51$, $p < 0.001$] connectivity was predictive of 3-month PCL-5 in women. However, only ITG-DMN connectivity [$t(28) = 3.89$, $\beta = 0.55$, $p < 0.001$], and not DLPFC-AN connectivity [$t(28) = -1.75$, $\beta = -0.30$, $p = 0.09$], was predictive of 3-month PCL-5 scores in men. These findings survived a Bonferroni correction for this set of analyses ($p = 0.05/4 = 0.013$).

In the present study, approximately 50% of participants reported hitting their head as part of the trauma that brought them into the ED. We therefore completed supplementary analyses to determine if potential concussion had an impact on the results. Participants who did not have a potential concussion showed DMN-ITG [$t(58) = 3.96$, $\beta = 0.47$, $p < 0.001$] and DLPFC-AN [$t(58) = -2.10$, $\beta = -0.27$, $p = 0.040$] connectivity with 3-month PTSD symptoms. Participants who did have a potential concussion showed DMN-ITG [$t(32) = 3.32$, $\beta = 0.49$, $p = 0.002$] and DLPFC-AN [$t(32) = -5.44$, $\beta = -0.69$, $p < 0.001$] connectivity with 3-month PTSD.

We also assessed specificity of the observed relationships with regard to race/ethnicity. Participants reported ethnicity as either a) Hispanic/latinx, b) White-American, c) Black-American, or d) “other.” Subgroup analyses were not performed for the “other” group as only five participants endorsed this category. DLPFC-AN connectivity was predictive of 3-month PCL-5 scores for White-American [$t(30) = -3.10$, $\beta = -0.53$, $p = 0.004$] and Black-American [$t(49) = -2.91$, $\beta = -0.39$, $p = 0.005$] participants, and was nearly significant for Hispanic/latinx participants

[$t(12) = -2.14$, $\beta = -0.56$, $p = 0.053$]. ITG-DMN connectivity was predictive of 3-month PCL-5 scores in White-American [$t(30) = 2.04$, $\beta = 0.36$, $p = 0.05$], Black-American [$t(49) = 4.90$, $\beta = 0.59$, $p < 0.001$], and Hispanic/latinx [$t(12) = 2.62$, $\beta = 0.60$, $p = 0.02$] participants. These results suggest the observed patterns of connectivity are predictive of later posttraumatic symptoms across racial groups. After a Bonferroni correction for this set of analyses, only DLPFC-AN connectivity in White-American and Black-American participants, as well as ITG-DMN connectivity predicting 3-month PCL-5 scores in Black-American participants, remained significant ($p = 0.05/6 = 0.008$).

Finally, although site was included as a covariate in the analyses, we completed follow-up regression analyses by site to explore if the observed effects were identifiable in each site individually. The number of participants recruited at each site varied considerably ($n_{\text{site1}} = 7$, $n_{\text{site2}} = 49$, $n_{\text{site3}} = 28$, $n_{\text{site4}} = 25$) and thus power to detect effects may have been limited for these analyses. DLPFC-AN connectivity was related to 3-month PCL-5 scores for site 2 [$t(47) = -5.11$, $\beta = -0.60$, $p < 0.001$] and site 3 [$t(26) = -2.12$, $\beta = -0.38$, $p = 0.04$], but not site 1 [$t(5) = -0.26$, $\beta = -0.11$, $p = 0.81$] or site 4 [$t(23) = -1.24$, $\beta = -0.25$, $p = 0.23$]. ITG-DMN connectivity was related to 3-month PCL-5 scores for site 2 [$t(47) = 4.54$, $\beta = 0.55$, $p < 0.001$] and site 4 [$t(23) = 2.67$, $\beta = 0.49$, $p = 0.01$], but not site 1 [$t(5) = 0.61$, $\beta = 0.26$, $p = 0.572$] or site 3 [$t(26) = 1.66$, $\beta = 0.31$, $p = 0.11$]. After a Bonferroni correction for this family of tests, only DLPFC-AN and ITG-DMN connectivity patterns for site 2 remained significant ($p = 0.05/8 = 0.006$).

Supplementary References

1. Esteban O, Markiewicz CJ, Blair RW, Moodie CA, Isik AI, Erramuzpe A, Kent JD, Goncalves M, DuPre E, Snyder M, Oya H, Ghosh SS, Wright J, Durnez J, Poldrack RA, Gorgolewski KJ. fMRIPrep: a robust preprocessing pipeline for functional MRI. *Nat Meth.* 2018; doi:[10.1038/s41592-018-0235-4](https://doi.org/10.1038/s41592-018-0235-4)
2. fMRIPrep Available from: [10.5281/zenodo.852659](https://zenodo.org/record/852659).
3. Gorgolewski K, Burns CD, Madison C, Clark D, Halchenko YO, Waskom ML, Ghosh SS. Nipype: a flexible, lightweight and extensible neuroimaging data processing framework in python. *Front Neuroinform.* 2011 Aug 22;5(August):13. doi:[10.3389/fninf.2011.00013](https://doi.org/10.3389/fninf.2011.00013).
4. Gorgolewski KJ, Esteban O, Ellis DG, Notter MP, Ziegler E, Johnson H, Hamalainen C, Yvernault B, Burns C, Manhães-Savio A, Jarecka D, Markiewicz CJ, Salo T, Clark D, Waskom M, Wong J, Modat M, Dewey BE, Clark MG, Dayan M, Loney F, Madison C, Gramfort A, Keshavan A, Berleant S, Pinsard B, Goncalves M, Clark D, Cipollini B, Varoquaux G, Wassermann D, Rokem A, Halchenko YO, Forbes J, Moloney B, Malone IB, Hanke M, Mordom D, Buchanan C, Pauli WM, Huntenburg JM, Horea C, Schwartz Y, Tungaraza R, Iqbal S, Kleesiek J, Sikka S, Frohlich C, Kent J, Perez-Guevara M, Watanabe A, Welch D, Cumba C, Ginsburg D, Eshaghi A, Kastman E, Bougacha S, Blair R, Acland B, Gillman A, Schaefer A, Nichols BN, Giavasis S, Erickson D, Correa C, Ghayoor A, Küttner R, Haselgrove C, Zhou D, Craddock RC, Haehn D, Lampe L, Millman J, Lai J, Renfro M, Liu S, Stadler J, Glatard T, Kahn AE, Kong X-Z, Triplett W, Park A, McDermottroe C, Hallquist M, Poldrack R, Perkins LN, Noel M, Gerhard S, Salvatore J, Mertz F, Broderick W, Inati S, Hinds O, Brett M, Durnez J, Tambini A, Rothmei S, Andberg SK, Cooper G, Marina A, Mattfeld A, Urchs S, Sharp P, Matsubara K, Geisler D, Cheung B, Floren A, Nickson T, Pannetier N, Weinstein A, Dubois M, Arias J, Tarbert C, Schlamp K, Jordan K, Liem F, Saase V, Harms R, Khanuja R, Podranski K, Flandin G, Papadopoulos Orfanos D, Schwabacher I, McNamee D, Falkiewicz M, Pellman J, Linkersdörfer J, Varada J, Pérez-García F, Davison A, Shachnev D, Ghosh S. Nipype: a flexible, lightweight and extensible neuroimaging data processing framework in Python. 2017. doi:[10.5281/zenodo.581704](https://doi.org/10.5281/zenodo.581704).
5. Tustison NJ, Avants BB, Cook PA, Zheng Y, Egan A, Yushkevich PA, Gee JC. N4ITK: improved N3 bias correction. *IEEE Trans Med Imaging.* 2010 Jun;29(6):1310–20. doi:[10.1109/TMI.2010.2046908](https://doi.org/10.1109/TMI.2010.2046908).
6. Dale A, Fischl B, Sereno MI. Cortical Surface-Based Analysis: I. Segmentation and Surface Reconstruction. *Neuroimage.* 1999;9(2):179–94. doi:[10.1006/nimg.1998.0395](https://doi.org/10.1006/nimg.1998.0395).
7. Fonov VS, Evans AC, McKinstry RC, Almlí CR, Collins DL. Unbiased nonlinear average age-appropriate brain templates from birth to adulthood. *NeuroImage; Amsterdam.* 2009 Jul 1;47:S102. doi:[10.1016/S1053-8119\(09\)70884-5](https://doi.org/10.1016/S1053-8119(09)70884-5).
8. Avants BB, Epstein CL, Grossman M, Gee JC. Symmetric diffeomorphic image registration with cross-correlation: evaluating automated labeling of elderly and neurodegenerative brain. *Med Image Anal.* 2008 Feb;12(1):26–41. doi:[10.1016/j.media.2007.06.004](https://doi.org/10.1016/j.media.2007.06.004).

9. Jenkinson M, Bannister P, Brady M, Smith S. Improved optimization for the robust and accurate linear registration and motion correction of brain images. *Neuroimage*. 2002 Oct;17(2):825–41. doi:[10.1006/nimg.2002.1132](https://doi.org/10.1006/nimg.2002.1132).
10. Andersson JLR, Skare S, Ashburner J. How to correct susceptibility distortions in spin-echo echo-planar images: application to diffusion tensor imaging. *Neuroimage*. 2003 Oct;20(2):870–88. doi:[10.1016/S1053-8119\(03\)00336-7](https://doi.org/10.1016/S1053-8119(03)00336-7).
11. Cox RW. AFNI: software for analysis and visualization of functional magnetic resonance neuroimages. *Comput Biomed Res*. 1996 Jun;29(3):162–73. doi:[10.1006/cbmr.1996.0014](https://doi.org/10.1006/cbmr.1996.0014).
12. Jenkinson M. Fast, automated, N-dimensional phase-unwrapping algorithm. *Magn Reson Med*. 2003 Jan;49(1):193–7. doi:[10.1002/mrm.10354](https://doi.org/10.1002/mrm.10354).
13. Huntenburg JM. Evaluating nonlinear coregistration of BOLD EPI and T1w images. Freie Universität Berlin; 2014. Available from: <http://hdl.handle.net/11858/00-001M-0000-002B-1CB5-A>.
14. Wang S, Peterson DJ, Gatenby JC, Li W, Grabowski TJ, Madhyastha TM. Evaluation of Field Map and Nonlinear Registration Methods for Correction of Susceptibility Artifacts in Diffusion MRI. *Front Neuroinform*. 2017 [cited 2017 Feb 21];11. doi:[10.3389/fninf.2017.00017](https://doi.org/10.3389/fninf.2017.00017).
15. Treiber JM, White NS, Steed TC, Bartsch H, Holland D, Farid N, McDonald CR, Carter BS, Dale AM, Chen CC. Characterization and Correction of Geometric Distortions in 814 Diffusion Weighted Images. *PLoS One*. 2016 Mar 30;11(3):e0152472. doi:[10.1371/journal.pone.0152472](https://doi.org/10.1371/journal.pone.0152472).
16. Greve DN, Fischl B. Accurate and robust brain image alignment using boundary-based registration. *Neuroimage*. 2009 Oct;48(1):63–72. doi:[10.1016/j.neuroimage.2009.06.060](https://doi.org/10.1016/j.neuroimage.2009.06.060).
17. Zhang Y, Brady M, Smith S. Segmentation of brain MR images through a hidden Markov random field model and the expectation-maximization algorithm. *IEEE Trans Med Imaging*. 2001 Jan;20(1):45–57. doi:[10.1109/42.906424](https://doi.org/10.1109/42.906424).
18. Behzadi Y, Restom K, Liao J, Liu TT. A component based noise correction method (CompCor) for BOLD and perfusion based fMRI. *Neuroimage*. 2007 Aug 1;37(1):90–101. doi:[10.1016/j.neuroimage.2007.04.042](https://doi.org/10.1016/j.neuroimage.2007.04.042).
19. Power JD, Mitra A, Laumann TO, Snyder AZ, Schlaggar BL, Petersen SE. Methods to detect, characterize, and remove motion artifact in resting state fMRI. *Neuroimage*. 2013 Aug 29;84:320–41. doi:[10.1016/j.neuroimage.2013.08.048](https://doi.org/10.1016/j.neuroimage.2013.08.048).
20. Pruim RHR, Mennes M, van Rooij D, Llera A, Buitelaar JK, Beckmann CF. ICA-AROMA: A robust ICA-based strategy for removing motion artifacts from fMRI data. *Neuroimage*. 2015 May 15;112:267–77. doi:[10.1016/j.neuroimage.2015.02.064](https://doi.org/10.1016/j.neuroimage.2015.02.064).

21. Klein A, Ghosh SS, Bao FS, Giard J, Häme Y, Stavsky E, et al. Mindboggling morphometry of human brains. *PLoS Comput Biol* 13(2): e1005350. 2017. doi:[10.1371/journal.pcbi.1005350](https://doi.org/10.1371/journal.pcbi.1005350).
22. Abraham A, Pedregosa F, Eickenberg M, Gervais P, Mueller A, Kossaifi J, Gramfort A, Thirion B, Varoquaux G. Machine learning for neuroimaging with scikit-learn. *Front in Neuroinf* 8:14. 2014. doi:[10.3389/fninf.2014.00014](https://doi.org/10.3389/fninf.2014.00014).
23. Pruim, R. H. R., Mennes, M., Buitelaar, J. K., & Beckmann, C. F. (2015). Evaluation of ICA-AROMA and alternative strategies for motion artifact removal in resting state fMRI. *NeuroImage*, 112, 278–287. <https://doi.org/10.1016/j.neuroimage.2015.02.063>
24. Pruim, R. H. R., Mennes, M., van Rooij, D., Llera, A., Buitelaar, J. K., & Beckmann, C. F. (2015). ICA-AROMA: A robust ICA-based strategy for removing motion artifacts from fMRI data. *NeuroImage*, 112, 267–277. <https://doi.org/10.1016/j.neuroimage.2015.02.064>
25. Satterthwaite, T. D., Ciric, R., Roalf, D. R., Davatzikos, C., Bassett, D. S., & Wolf, D. H. (2019). Motion artifact in studies of functional connectivity: Characteristics and mitigation strategies. *Human Brain Mapping*. <https://doi.org/10.1002/hbm.23665>
26. Esteban, O., Birman, D., Schaer, M., Koyejo, O. O., Poldrack, R. A., & Gorgolewski, K. J. (2017). MRIQC: Advancing the automatic prediction of image quality in MRI from unseen sites. *PLoS One*, 12(9), e0184661. <https://doi.org/10.1371/journal.pone.0184661>
27. Power, J. D., Barnes, K. A., Snyder, A. Z., Schlaggar, B. L., & Petersen, S. E. (2012). Spurious but systematic correlations in functional connectivity MRI networks arise from subject motion. *NeuroImage*, 59(3), 2142–2154. <https://doi.org/10.1016/j.neuroimage.2011.10.018>

Table S1. Additional demographic and participant information.

Injury Severity	
<i>ISS Score</i>	2.26 (1.55)
<i>Chance of dying</i>	5.07 (3.43)
Head injury	
<i>Yes</i>	49 (45%)
<i>No</i>	51 (47%)
<i>Missing</i>	9 (8%)
Potential Concussion	
<i>Yes</i>	37 (34%)
<i>No</i>	63 (58%)
<i>Missing</i>	9 (8%)
ED Psychiatric Symptoms	
<i>PCL-5 (n = 65)</i>	31.85 (15.62)
<i>PROMIS depression (n = 109)</i>	49.08 (10.48)

Note: ISS = Injury Severity Score; ED = Emergency Department; Values are Mean (Standard Deviation) or Count (Percentage)

Table S2. Broad trauma classifications in the present sample.

Traumatic event	Count
Motor vehicle collision	85
Physical assault	14
Sexual assault	2
Fall (≥ 10 feet)	1
Non-motorized collision	1
Fall (< 10 feet)	4
Burn	1
Animal-related	1

Table S3. Medication and substance use two-weeks following trauma.

Medications (n = 104)	Count
<i>Acetaminophen</i>	5
<i>ACE Inhibitor</i>	8
<i>Antibiotics</i>	7
<i>Anticholinergics</i>	9
<i>Benzodiazepines</i>	3
<i>Beta blockers</i>	1
<i>Contraceptives</i>	2
<i>Opioids</i>	8
<i>NSAIDs</i>	17
<i>SNRIs</i>	4
<i>SSRIs</i>	6
Substance use frequency in past 2-weeks (n =104)	Mean (Standard Deviation)
<i>Alcohol</i>	1.37 (2.43)
<i>Marijuana</i>	2.30 (4.61)
<i>Cocaine</i>	0.12 (0.99)
<i>Hallucinogens</i>	0.00 (0.01)
<i>Heroin</i>	0.00 (0.00)
<i>Opiates</i>	0.16 (1.40)
<i>Barbiturates</i>	0.04 (0.39)
<i>Sedatives</i>	0.16 (1.38)
<i>Stimulants</i>	0.00 (0.00)

Table S4. MRI scan sequence parameters by site.

	SITE1 SIEMENS TIM 3T TRIO (12 CHANNEL HEAD COIL)	SITE2 SIEMENS TIM 3T TRIO (12 CHANNEL HEAD COIL)	SITE3 SIEMENS MAGNETOM 3T PRISMA (20 CHANNEL HEAD COIL)	SITE4 SIEMENS 3T VERIO (12 CHANNEL HEAD COIL)
MODALITY				
T1- WEIGHTED	TR = 2530ms, TE_s = 1.74/3.6/5.46/7.32ms, TI = 1260ms, flip angle = 7, FOV = 256mm, slices = 176, Voxel size = 1mm x 1mm x 1mm	TR = 2530ms, TE_s = 1.74/3.6/5.46/7.32ms, TI = 1260ms, flip angle = 7, FOV = 256mm, slices = 176, Voxel size = 1mm x 1mm x 1mm	TR = 2300ms, TE = 2.96ms, TI = 900ms, flip angle = 9, FOV = 256mm, slices = 176, Voxel size = 1.2mm x 1.0mm x 12mm	TR = 2530ms, TE_s = 1.74/3.65/5.51/7.72ms, TI = 1260ms, flip angle = 7, FOV = 256mm, slices = 176, Voxel size = 1mm x 1mm x 1mm
FUNCTIONAL MRI	TR = 2360ms, TE = 30ms, flip angle = 70, FOV = 212mm, slices = 44, Voxel size = 3mm x 2.72mm x 2.72mm, 0.5 mm gap	TR = 2360ms, TE = 30ms, flip angle = 70, FOV = 212mm, slices = 44, Voxel size = 3mm x 3mm x 3mm, 0.5 mm gap	TR = 2360ms, TE = 29ms, flip angle = 70, FOV = 212mm, slices = 44, Voxel size = 3mm x 2.72mm x 2.72mm, 0.5 mm gap	TR = 2360ms, TE = 30ms, flip angle = 70, FOV = 212mm, slices = 42, Voxel size = 3mm x 2.72mm x 2.72mm, 0.5 mm gap

Table S5. Whole-brain analyses of network-to-node connectivity associated with 3-month posttraumatic stress severity when controlling for 2-week symptoms.

	Hemisphere	Z-Statistic	Volume	Coordinates (MNI) X, Y, Z
<u>Arousal network</u>				
Postcentral Gyrus	Right	-4.36	$k = 57$ (456 mm ³)	38, -31, 44
Visual cortex	Right	-4.61	$k = 46$ (368 mm ³)	14, -97, -11

Note: Location, Z-Statistic, volume (in cluster extent, k ; 2³mm grid spacing), volume, and Montreal Neurological Institute (MNI) coordinates of the peak voxel for clusters that showed a significant ($\alpha = 0.05$; corrected) relationship with 3-month PCL-5 (PTSD CheckList for DSM-V) scores when controlling for 2-week PCL-5 scores.

Figure S1. **Sitewise differences in quality assurance metrics.** Differences in the AFNI Quality Index (AQI), Framewise Displacement (FD), DVARs, and temporal signal-to-noise ratio (TSNR) were calculated between each neuroimaging site. Gray bars reflect the mean value of each metric per site, and the error bars reflect the standard error of the mean.

